Research Article Vol. 28, No. 10 / 11 May 2020 / Optics Express 14263
Optics EXPRESS

Fiber-interface directional coupler inscribed by femtosecond laser for refractive index measurements

JINLI HAN,[1,2] YUNFANG ZHANG,[1,2] CHANGRUI LIAO,[1,2,*] YUYING JIANG,[1,2] YING WANG,[1,2] CHUPAO LIN,[1,2] SHEN LIU,[1,2] JIACHEN WANG,[1,2] ZHE ZHANG,[1,2] JIANGTAO ZHOU,[3] AND YIPING WANG[1,2]

[1]*Guangdong and Hong Kong Joint Research Centre for Optical Fibre Sensors, College of Physics and Optoelectronic Engineering, Shenzhen University, Shenzhen 518060, China*
[2]*Key Laboratory of Optoelectronic Devices and Systems of Ministry of Education and Guangdong Province, Shenzhen University, Shenzhen 518060, China*
[3]*Laboratory of Physics of Living Matter, Ecole Polytechnique Fédérale de Lausanne (EPFL), Lausanne 1015, Switzerland*
[*]*cliao@szu.edu.cn*

Abstract: A novel fiber-interface directional waveguide coupler was inscribed on the surface of a coreless fiber by femtosecond laser, and was successfully applied to highly sensitive refractive index (RI) measurements. The primary arm was first inscribed to couple light from a lead-in single mode fiber to the fiber interface, then back to a lead-out single mode fiber. A side arm was inscribed parallel and in close proximity to the primary arm. Light propagating in the primary arm could then be efficiently coupled into the side arm when a phase-matching condition was met, which produced a dramatic spectral dip at the coupling wavelength. The proposed device achieved a sensitivity as high as ~8249 nm/RIU over an RI range of 1.44-1.45, due to strong evanescent fields excited in fiber-interface waveguides. The proposed in-fiber directional coupler exhibits high mechanical strength, a compact configuration, and excellent RI sensitivity. As such, it has significant potential for practical applications in biochemical sensing.

1. Introduction

Optical fiber-based refractive index sensors have shown significant potential for biochemical applications due to advantages such as a compact size, fast response, and immunity to electromagnetic interference [1–3]. Microfiber directional couplers (MFCs), a specific type of micro-optic device, have been widely used in liquid refractive index (RI) sensing [4–7]. These devices have achieved sensitivities as high as 4155 nm/RIU by measuring interactions between evanescent fields leaking from silica fibers and the surrounding medium [4]. However, conventional MFCs are often fabricated by fusing and tapering two adjacent fibers, which often leads to low machining repeatability and poor mechanical strength. As such, a novel design offering increased durability, accuracy, and design repeatability would be highly beneficial for ensuring strong evanescent fields of the optical waveguide (WG).

Direct femtosecond (FS) laser inscription provides a viable solution as it is capable of forming precise optical waveguides in glass with high flexibility and spatial accuracy [8–12]. FS lasers have been successfully used to inscribe waveguides in fiber claddings, near the center of the fiber [13–16]. Our group has previously proposed a fiber-interface waveguide configuration and, since 2017, has successfully produced several fiber sensors based on a surface waveguide. This has included fiber-surface Bragg grating, fiber-interface Mach-Zehnder interferometer, and surface plasmon resonance devices [17–19]. In these studies, the waveguides fabricated on the cladding

#390674 https://doi.org/10.1364/OE.390674
Journal © 2020 Received 17 Feb 2020; revised 19 Apr 2020; accepted 19 Apr 2020; published 27 Apr 2020

Optics EXPRESS

interface supported light propagation with enhanced evanescent fields, providing a new technique for RI measurements.

In this study, we demonstrate a fiber-interface directional coupler, as a research continuing of Ref. [18], which was fabricated in a coreless fiber spliced between two single mode fibers (SMFs). As shown in Fig. 1, a U-shaped waveguide (WG_1) was first fabricated as the primary arm. It was formed using two s-bend waveguides and a straight waveguide, which transfers light from the lead-in SMF to the fiber interface and then back to the lead-out SMF. The other straight waveguide (WG_2), forming the side arm, was fabricated parallel to WG_1 at a distance of ~6 μm. As light propagates into the straight section of WG_1, a fraction of the signal is coupled into WG_2 when a phase-matching condition is met [16,20,21]. The light propagating into WG_2 cannot be recoupled back to WG_1 and will eventually be emitted into the cladding, resulting in a transmission loss. The proposed fiber-interface directional coupler exhibits a high sensitivity of ~8249 nm/RIU over an RI range of 1.44-1.45. In addition, the waveguide is non-destructively inscribed inside the fiber, preventing damage to the exterior and ensuring high mechanical strength.

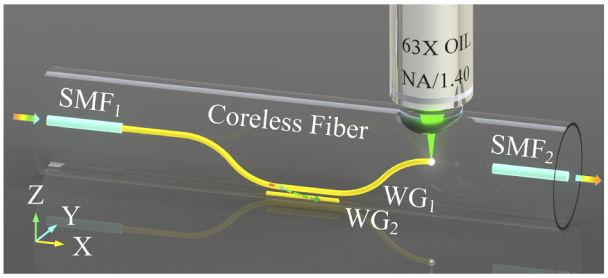

Fig. 1. A schematic diagram of the femtosecond laser-inscribed fiber-interface directional coupler.

2. Device fabrication

A device fabrication flowchart is shown in Fig. 2. In this process, a section of the coreless fiber is spliced with two SMFs (Corning, SMF-28). This provides a platform for fabrication of the U-shaped waveguide (WG_1), which is inscribed in a coreless fiber and connects the cores of two SMFs. The two ends of WG_1 are then stretched into the cores of two SMFs over a length of ~15 μm (L_1), to increase the coupling efficiency. The radius of the curved components (R) is set at 50 mm to decrease bending loss in WG_1. The optimal parameters of L_1 and R, adopted in this paper, have been demonstrated in [18]. The straight waveguide (WG_2) was inscribed parallel to WG_1.

During inscription, a femtosecond laser (PHAROS, 513 nm/290 fs/200 kHz) was used to inscribe the waveguides and an oil-immersed objective lens (NA = 1.4) was included to eliminate aberrations caused by the cylindrical fiber morphology. The fixed fiber was then translated relative to the focused laser beam via a 3D air-bearing motion stage (Aerotech). The laser pulse energy was optimized at ~120 nJ and the translational velocity of the fiber was set to 200 μm/s. Propagation loss of the inscribed waveguide of ~0.1 dB/mm and coupling loss at the joint point of ~0.6 dB have been demonstrated by Zhang et al. under the same laser inscription parameters [18].

Figure 3(a) shows a top-view optical microscope image of fiber-interface directional coupler, corresponding to the coupling region in Fig. 2(d), two parallel waveguides were inscribed horizontally with a separation of ~6 μm. This distance is critical for ensuring adequate coupling efficiency, which increases as the distance between the waveguides decreases. An insufficient separation may lead to overlapping, which can diminish performance [11]. The length of WG_2

Optics EXPRESS

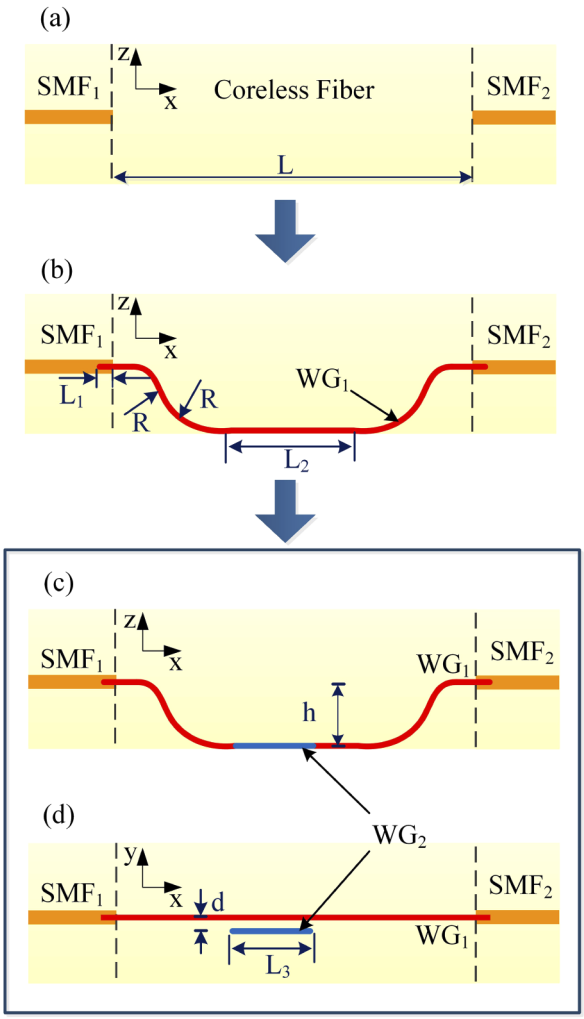

Fig. 2. A flowchart of the device fabrication process. (a) The coreless fiber was spliced between two SMFs. (b) WG_1 was inscribed in the coreless fiber. WG_2 was inscribed parallel to WG_1 with a separation distance of d from side-view (c) and top-view (d). Optimized parameters included: L = 10.6 mm, L_1=15 µm, R = 50 mm, L_2=3.7 mm, h = 60.8 µm, d = 6 µm and L_3=3 mm.

was optimized at 3 mm to achieve a significant directional coupling dip for improved sensing capabilities. The fabricated device was connected to an amplified spontaneous emission (ASE) light source and the transmission spectrum was measured using an optical spectrum analyzer (OSA). As shown in Fig. 3(b), transmission dips were produced by directional coupling between WG_1 and WG_2. The intensities of dip A and dip B were measured to be ~12.7 dB and ~12.5 dB, respectively. The intensities of other coupling dips are not as strong as dip A and dip B that can be explained by the spectra superposition and compensation of the two orthogonal polarization modes.

A cross-sectional view of the coreless fiber embedded with a directional coupler is shown in Fig. 4, where the Fs laser, incident from the top surface, inscribed two waveguides at the bottom of the fiber interface. To enhance the evanescent field of the waveguides, the laser beam was

Optics EXPRESS

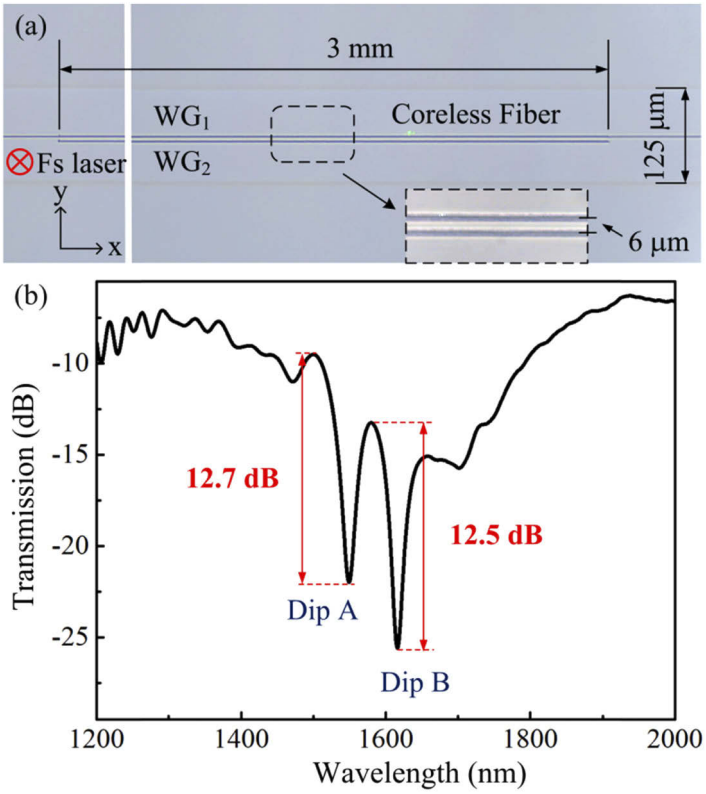

Fig. 3. (a) An optical microscope image of the top view of the fiber-interface directional coupler, with WG_1 and WG_2 inscribed by a femtosecond laser with incident direction perpendicular to XY plane. The inset figure provides a high-magnification image of the waveguides. (b) The transmission spectrum of the fiber-interface directional coupler.

focused at different distances away from the center of the fiber. When the focal spot, is ~60.8 μm away from the center of the fiber, it ensures the waveguide very close to but not beyond the fiber surface. The size of these two waveguides is ~14 μm in depth and ~3 μm in width. There are segments of both negative (black) and positive (white) RI modifications in the laser inscribed

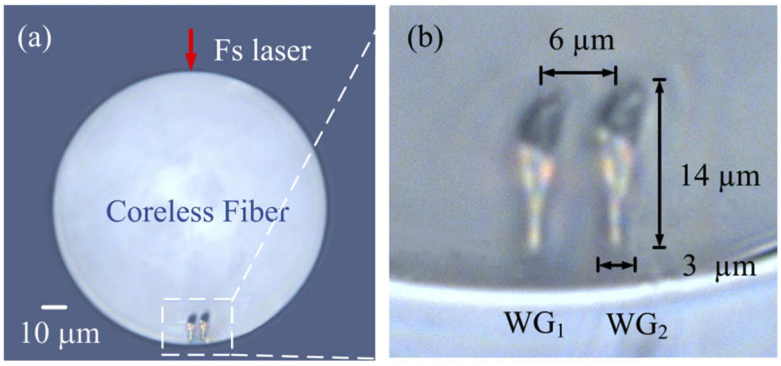

Fig. 4. (a) An optical microscope image of the fiber-interface directional coupler cross-section. (b) Magnification of the waveguides region.

Optics EXPRESS

waveguide, and the focal spot of the laser beam is located at the positive RI modification area [18,22].

The RI distribution of the laser-inscribed waveguide is further studied by a 3D reconstruction system [23]. The cross-sectional RI distribution of a single laser-inscribed waveguide is clearly presented in Fig. 5, where it consists of both negative and positive RI modulation segments. The largest magnitude of the negative RI modulation is measured to be $\sim 3\times10^{-2}$, and the positive RI modulation is up to $\sim 5\times10^{-3}$, which ensures good confinement of the guided light.

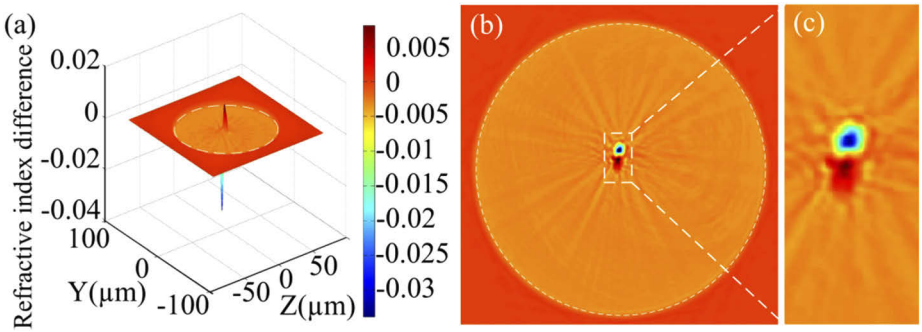

Fig. 5. (a) Three dimensional and (b) two dimensional cross-sectional RI difference diagrams of the laser-waveguide. The dotted circle indicates the boundary of the coreless fiber. (c) Magnification of the waveguide region.

3. Device characterization and discussion

The mode profile of WG_1 and WG_2 was tested using a tunable laser light source (Agilent, Model 81940A) and a camera (Newport, LBP2-HR-IR2). The output facet, used for mode profile testing, is the end of the coupling region for the directional coupler, which is prepared by cutting off another sample fabricated with the same parameters. These two cases are illustrated in Fig. 6, which shows light coupling between the two waveguides. When light at 1520 nm is incident in the coupler, as shown in Fig. 6(a), most of the power is located within WG_2. As the wavelength of incident light is increased to 1533.7 nm, as shown in Fig. 6(b), the center of the power profile shifts toward WG_1. Light coupling between WG_1 and WG_2 then occurs via the evanescent field. Figure 6 demonstrates that mode coupling between the fiber-interface waveguides occurs over a wide range of wavelengths, due to comparable material dispersion.

The RI response of the fiber-interface directional coupler was investigated at room temperature by immersing the device in a series of standard liquids (Cargille Labs) with RI values increasing from 1.440 to 1.450 in increments of 0.002. An additional rinsing step was included before each measurement to ensure the fiber surface was cleaned completely. The evolution of the transmission spectrum for dip B in Fig. 3(b) is plotted in Fig. 7(a). The measured dip wavelength was fitted as an exponential function of the surrounding RI. Results showed that its sensitivity increased significantly as the surrounding RI value approached that of the fiber cladding, due to an enhanced evanescent field. The fiber-interface directional coupler exhibited an average RI sensitivity as high as 8249 nm/RIU over an RI range of 1.44-1.45. A maximum sensitivity of ~16983 nm/RIU was achieved at 1.45.

The influence of temperature on the fiber-interface directional coupler was also investigated by placing it in an electric oven. A heating treatment was applied over a range of 25–95 °C, as depicted in Fig. 8(a). A blue shift was observed in dip B as the temperature increased. The relationship between dip wavelength and temperature is presented in Fig. 8(b), where the data

Optics EXPRESS

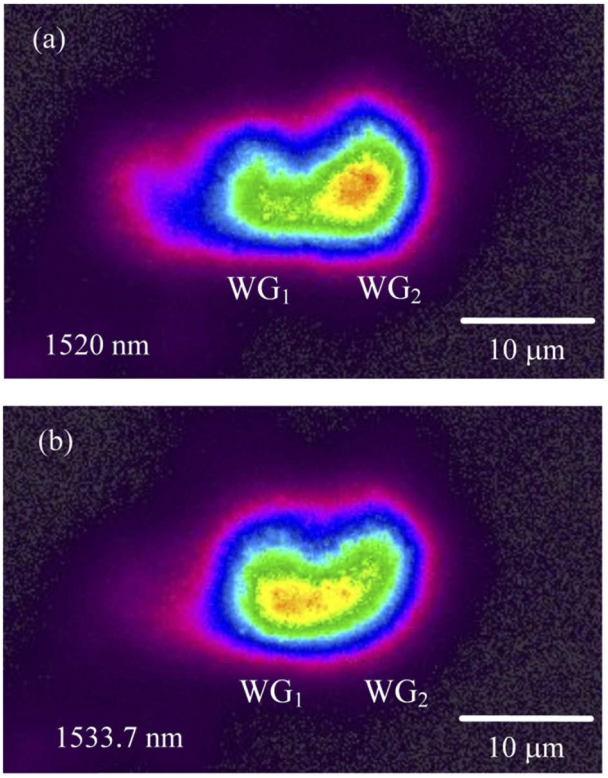

Fig. 6. The mode profile of the fiber-interface directional coupler at (a) 1520 nm and (b) 1533.7 nm.

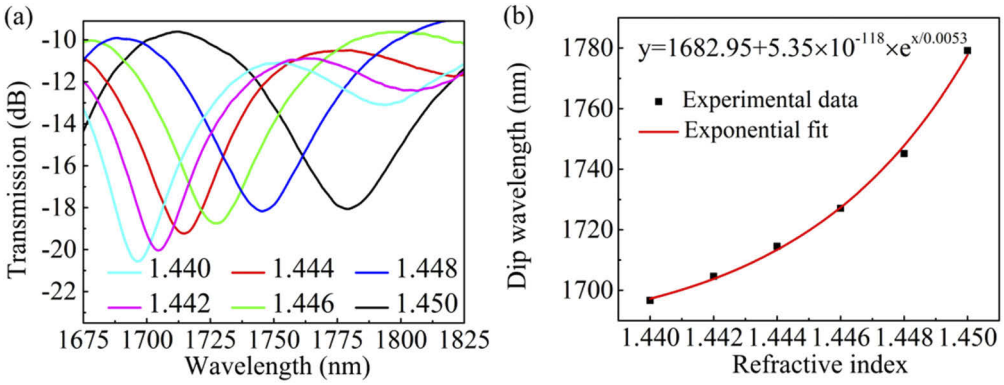

Fig. 7. The liquid RI response of the fiber-interface directional coupler. (a) The transmission spectra produced by the device when immersed in different RI liquids. (b) The exponential relationship between the wavelength of the coupling dip and the RI of the liquid.

exhibit a linear relationship and the temperature sensitivity was calculated to be ~15 pm/°C. This value is small enough to be neglected during RI measurements.

In addition, the mechanical strength of the coupler was investigated experimentally. First, a series of bending resistance tests were conducted by bending the device 360° along marker pens with varying diameters (all >20 mm). Secondly, a strain limitation test was conducted

Optics EXPRESS

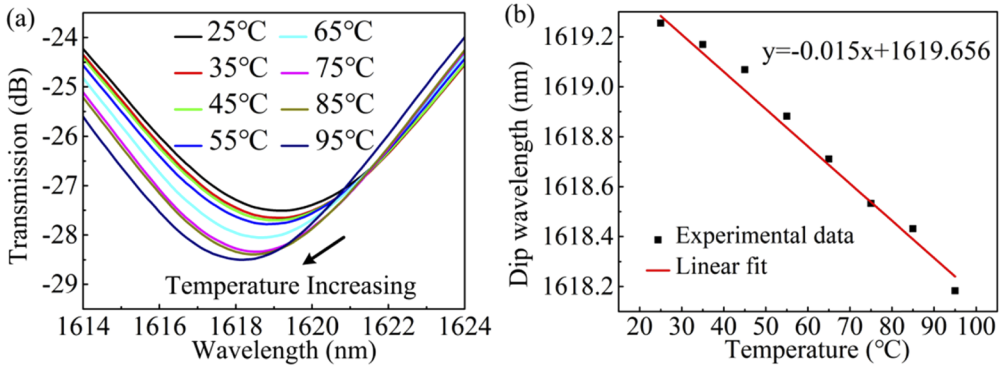

Fig. 8. (a) Transmission spectra evolution for the proposed device as the temperature increased from 25–95°C. (b) The relationship between temperature and dip wavelength.

by stretching the coupler until it broke, yielding a maximum strain of 5450 με. These results confirm negligible degradation of fiber mechanical strength after femtosecond laser inscription.

4. Conclusion

A fiber-interface directional coupler was produced using direct femtosecond laser inscription for application to refractive index sensing. This coupler can measure the RI of a surrounding medium without requiring any chemical etching or tapering of the fiber. The device also exhibits a high sensitivity of ~8249 nm/RIU over an RI range of 1.44-1.45. Its temperature sensitivity is as low as 15 pm/°C, allowing temperature cross-sensitivity to be neglected during RI measurements. As a practical RI sensor, this fiber-interface directional coupler exhibits several advantageous mechanical properties, such as simple and repeatable fabrication, excellent mechanical strength, ultra-high RI sensitivity, and low temperature cross-sensitivity. As such, it could be a valuable new tool for applications in trace biochemical detection.

Funding

National Natural Science Foundation of China (61575128, 61635007); Natural Science Foundation of Guangdong Province (2014A030308007, 2018B030306003); Science, Technology and Innovation Commission of Shenzhen Municipality (JCYJ20160427104925452, JCYJ20170818093743767, KQJSCX20170727101953680); Development and Reform Commission of Shenzhen Municipality.

Acknowledgments

The authors acknowledge the Photonics Center of Shenzhen University for providing the Femtosecond Laser Micromachining System to inscribe the waveguides.

Disclosures

The authors declare no conflicts of interest.

References

1. K. Grattan and T. Sun, "Fiber optic sensor technology: an overview," Sens. Actuators, A **82**(1-3), 40–61 (2000).
2. C. Caucheteur, T. Guo, F. Liu, B. O. Guan, and J. Albert, "Ultrasensitive plasmonic sensing in air using optical fibre spectral combs," Nat. Commun. **7**, 13371 (2016).

Optics EXPRESS

3. C. Gong, Y. Gong, X. Zhao, Y. Luo, Q. Chen, X. Tan, Y. Wu, X. Fan, G. Peng, and Y. Rao, "Distributed fibre optofluidic laser for chip-scale arrayed biochemical sensing," Lab Chip **18**, 2741–2748 (2018).
4. L. Bo, P. Wang, Y. Semenova, and G. Farrell, "High sensitivity fiber refractometer based on an optical microfiber coupler," IEEE Photonics Technol. Lett. **25**(3), 228–230 (2013).
5. C. R. Liao, D. N. Wang, X. Y. He, and M. W. Yang, "Twisted optical microfibers for refractive index sensing," IEEE Photonics Technol. Lett. **23**(13), 848–850 (2011).
6. Y. Jung, G. Brambilla, and D. J. Richardson, "Optical microfiber coupler for broadband single-mode operation," Opt. Express **17**(7), 5273–5278 (2009).
7. R. Ismaeel, T. Lee, B. Oduro, Y. Jung, and G. Brambilla, "All-fiber fused directional coupler for highly efficient spatial mode conversion," Opt. Express **22**(10), 11610–11619 (2014).
8. L. A. Fernandes, J. R. Grenier, P. V. S. Marques, J. S. Aitchison, and P. R. Herman, "Strong birefringence tuning of optical waveguides with femtosecond laser irradiation of bulk fused silica and single mode fibers," J. Lightwave Technol. **31**(22), 3563–3569 (2013).
9. C. Waltermann, A. Doering, M. Köhring, M. Angelmahr, and W. Schade, "Cladding waveguide gratings in standard single-mode fiber for 3D shape sensing," Opt. Lett. **40**(13), 3109–3112 (2015).
10. X. Yang, W. Shu, Y. Wang, Y. Gong, C. Gong, Q. Chen, X. Tan, G. D. Peng, X. Fan, and Y. J. Rao, "Turbidimetric inhibition immunoassay revisited to enhance its sensitivity via an optofluidic laser," Biosens. Bioelectron. **131**, 60–66 (2019).
11. J. R. Grenier, L. A. Fernandes, and P. R. Herman, "Femtosecond laser inscription of asymmetric directional couplers for in-fiber optical taps and fiber cladding photonics," Opt. Express **23**(13), 16760–16771 (2015).
12. P. Ji, S. U. Baek, C. H. Park, S. S. Lee, Y. E. Im, and Y. Choi, "Inline fiber optic power sensor featuring a variable tap ratio based on a tightly focused femtosecond laser inscription," Opt. Express **26**(12), 14972 (2018).
13. K. K. C. Lee, A. Mariampillai, M. Haque, B. A. Standish, V. X. D. Yang, and P. R. Herman, "Temperature-compensated fiber-optic 3D shape sensor based on femtosecond laser direct-written Bragg grating waveguides," Opt. Express **21**(20), 24076–24086 (2013).
14. W. W. Li, W. P. Chen, D. N. Wang, Z. K. Wang, and B. Xu, "Fiber inline Mach-Zehnder interferometer based on femtosecond laser inscribed waveguides," Opt. Lett. **42**(21), 4438–4441 (2017).
15. B. Huang and X. Shu, "Highly sensitive torsion sensor with femtosecond laser-induced low birefringence single-mode fiber based Sagnac interferometer," Opt. Express **26**(4), 4563–4571 (2018).
16. C. Lin, C. Liao, Y. Zhang, L. Xu, Y. Wang, C. Fu, K. Yang, J. Wang, J. He, and Y. Wang, "Optofluidic gutter oil discrimination based on a hybrid-waveguide coupler in fiber," Lab Chip **18**(4), 595–600 (2018).
17. C. Lin, C. Liao, J. Wang, J. He, Y. Wang, Z. Li, T. Yang, F. Zhu, K. Yang, Z. Zhang, and Y. Wang, "Fiber surface Bragg grating waveguide for refractive index measurements," Opt. Lett. **42**(9), 1684–1687 (2017).
18. Y. Zhang, C. Lin, C. Liao, K. Yang, Z. Li, and Y. Wang, "Femtosecond laser-inscribed fiber interface Mach-Zehnder interferometer for temperature-insensitive refractive index measurement," Opt. Lett. **43**(18), 4421–4424 (2018).
19. Y. Zhang, C. Liao, C. Lin, Y. Shao, Y. Wang, and Y. Wang, "Surface plasmon resonance refractive index sensor based on fiber-interface waveguide inscribed by femtosecond laser," Opt. Lett. **44**(10), 2434–2437 (2019).
20. C. Lin, Y. Wang, Y. Huang, C. Liao, Z. Bai, M. Hou, Z. Li, and Y. Wang, "Liquid modified photonic crystal fiber for simultaneous temperature and strain measurement," Photonics Res. **5**(2), 129–133 (2017).
21. Y. Wang, C. R. Liao, and D. N. Wang, "Femtosecond laser-assisted selective infiltration of microstructured optical fibers," Opt. Express **18**(17), 18056–18060 (2010).
22. P. Ji, S. S. Lee, Y. E. Im, and Y. Choi, "Determination of geometry-induced positional distortion of ultrafast laser-inscribed circuits in a cylindrical optical fiber," Opt. Lett. **44**(3), 610–613 (2019).
23. C. Yan, S. J. Huang, Z. Miao, Z. Chang, J. Z. Zeng, and T. Y. Wang, "3D refractive index measurements of special optical fibers," Opt. Fiber Technol. **31**, 65–73 (2016).